

in the mole fraction range $X_{V_2O_5} = 0.22-0.33$ is considered a realistic description of the catalyst. However, the temperature of the melt should be in the range 400–500 °C, and furthermore the melt should be in contact with an $SO_2/O_2/SO_3$ gas mixture in order to correspond to the conditions of operation. Even in the absence of this redox mixture the complexes of vanadium(V) in the $V_2O_5-K_2S_2O_7$ binary system might very well be analogous to the complexes formed during operation of the catalyst. The present results show that the dominating vanadium(V) complex in solution in the mole fraction range $X_{V_2O_5} = 0.22-0.33$ is probably the dimer $(VO_2)_2(SO_4)_2S_2O_7^{4-}$. Furthermore, the results for the ternary $V_2O_5-K_2S_2O_7-K_2SO_4$ system show that the $S_2O_7^{2-}$ group is labile and that a ligand exchange forming $(VO_2)_2(SO_4)_3^{4-}$ can take place. This lability might lead to an exchange of $S_2O_7^{2-}$ with SO_2 during the catalytic reaction, giving rise to the formation of the complex $(VO_2)_2(SO_4)_2SO_2^{2-}$ as the initial step in the catalytic cycle. In this complex a two-electron transfer from SO_2 to the vanadium central atoms forming SO_3 and possibly a V(IV) complex might take place simultaneously.

The redox and complex chemistry of vanadium in similar melts is under investigation.²⁵⁻²⁷ Furthermore, an extended calorimetric

(25) Fehrmann, R.; Hansen, N. H.; Bjerrum, N. J.; Phillipsen, J.; Pedersen, E., to be submitted for publication.

study involving temperatures other than 430 °C in the range 400–450 °C is under way;²⁸ conductivity and density measurements are in progress.¹⁸

Acknowledgment. The authors wish to thank Dr. J. P. Bros (UP) for helpful discussions and Dr. G. Hatem (UP) for experimental help. Further thanks are due the Danish Technical Science Research Foundation and Université de Provence for financial support. This investigation has been carried out within the program of "Stimulation Actions" of the European Economic Community in accordance with Contract No. STI-011-J-C(CD).

Registry No. KVO_2SO_4 , 67163-79-5; $K_4(VO_2)_2(SO_4)_2S_2O_7$, 76569-58-9; $K_3VO_2SO_4S_2O_7$, 76569-57-8; V_2O_5 , 1314-62-1; $K_2S_2O_7$, 7790-62-7; K_2SO_4 , 7778-80-5.

Supplementary Material Available: Listings of experimental values of molar liquid-liquid enthalpies of mixing for the system $V_2O_5-K_2S_2O_7$ at 430 °C (Table I) and for the three different pseudobinary compositions of the ternary system $V_2O_5-K_2S_2O_7-K_2SO_4$ at 430 °C (Table II) (5 pages). Ordering information is given on any current masthead page.

(26) Fehrmann, R.; Papatheodorou, G. N.; Bjerrum, N. J., to be submitted for publication.

(27) Fehrmann, R.; Krebs, B.; Papatheodorou, G. N.; Berg, R. W.; Bjerrum, N. J. *Inorg. Chem.*, in press.

(28) Fehrmann, R.; Jeanne, P.; Gaune-Escard, M.; Bjerrum, N. J., to be submitted for publication.

Contribution from the Guelph Waterloo Centre for Graduate Work in Chemistry, Guelph Campus, Department of Chemistry and Biochemistry, University of Guelph, Guelph, Ontario N1G 2W1, Canada, and Department of Chemistry, University of Arkansas, Fayetteville, Arkansas 72701

Aromatic and Antiaromatic Thiazyl Heterocycles. Comparison of the Structural, Spectroscopic, and Cycloaddition Properties of 1,3,2,4-Benzodithiadiazine, $C_6H_4S_2N_2$, and 1,3,5,2,4-Benzotrithiadiazepine, $C_6H_4S_3N_2$

A. Wallace Cordes,^{1a} Masashi Hojo,^{1b,c} Hans Koenig,^{1b} Mark C. Noble,^{1a} Richard T. Oakley,^{*1b} and William T. Pennington^{1a}

Received August 5, 1985

Preparative routes to 1,3,2,4-benzodithiadiazine, $C_6H_4S_2N_2$, 1,3,5,2,4-benzotrithiadiazepine, $C_6H_4S_3N_2$, and their respective norbornadiene adducts $C_6H_4S_2N_2 \cdot C_7H_8$ and $C_6H_4S_3N_2 \cdot C_7H_8$ are described. The molecular structures of $C_6H_4S_2N_2$ and the two adducts have been determined by X-ray crystallography. The structural differences between $C_6H_4S_2N_2$ and $C_6H_4S_3N_2$ are related to MNDO molecular orbital calculations on their ground-state electronic structures. The aromatic/antiaromatic characters of the two compounds are discussed in relation to their electronic and ¹H NMR spectra, their electrochemical behavior, and the ease of dissociation of their norbornadiene adducts. Crystal data for $C_6H_4S_2N_2$: monoclinic, space group *Pc*, $a = 5.616$ (1) Å, $b = 3.896$ (1) Å, $c = 15.434$ (3) Å, $\beta = 102.23$ (2)°, $V = 330.0$ Å³, $Z = 2$ at -115 °C, $R = 0.040$ for 634 reflections with $I > 3\sigma(I)$. Crystal data for $C_6H_4S_2N_2 \cdot C_7H_8$: orthorhombic, space group *Pbca*, $a = 10.230$ (3) Å, $b = 19.922$ (7) Å, $c = 11.221$ (6) Å, $V = 2309$ Å³, $Z = 8$ at 20 °C, $R = 0.044$ for 1175 reflections with $I > 3\sigma(I)$. Crystal data for $C_6H_4S_3N_2 \cdot C_7H_8$: orthorhombic, space group *Pbca*, $a = 10.571$ (2) Å, $b = 11.914$ (2) Å, $c = 20.027$ (3) Å, $V = 2522$ Å³, $Z = 8$ at 21 °C, $R = 0.040$ for 2034 reflections with $I > 3\sigma(I)$.

Introduction

The electronic structures of planar binary sulfur-nitrogen rings and related derivatives have been the subjects of many theoretical studies,² most of which have focused attention on the structural consequences of the occupation of antibonding π orbitals³ and on

the interpretation of their electronic⁴ and MCD⁵ spectra. One intriguing question regarding these compounds concerns the relevance of the term aromaticity in discussing their chemical properties. The preponderance of planar cyclic $4n + 2$ π -systems, e.g. $S_5N_5^+$, $S_4N_4^{2+}$, $S_4N_3^+$, $S_3N_3^-$, S_2N_2 , provides an appealing argument for the applicability of the Hückel rule. However, more detailed studies of the potential analogies between these inorganic

(1) (a) University of Arkansas. (b) University of Guelph. (c) Permanent address: Department of Chemistry, Faculty of Science, Kochi University, Kochi 780, Japan.

(2) For recent reviews see: (a) Chivers, T. *Acc. Chem. Res.* **1984**, *17*, 166. (b) Chivers, T.; Oakley, R. T. *Top. Curr. Chem.* **1982**, *102*, 117. (c) Gleiter, R. *Angew. Chem., Int. Ed. Engl.* **1981**, *20*, 444. (d) Chivers, T. *Chem. Rev.* **1985**, *85*, 341.

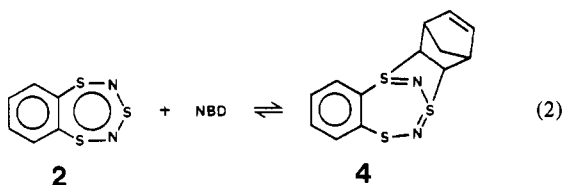
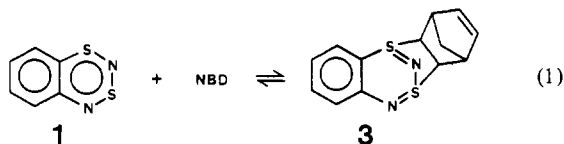
(3) (a) Gleiter, R.; Bartetzko, R.; Cremer, D. *J. Am. Chem. Soc.* **1984**, *106*, 3437. (b) Oakley, R. T. *Can. J. Chem.* **1984**, *62*, 2763. (c) Marcellus, C. G.; Oakley, R. T.; Cordes, A. W.; Pennington, W. T. *Can. J. Chem.* **1984**, *62*, 1822. (d) Cordes, A. W.; Marcellus, C. G.; Noble, M. C.; Oakley, R. T.; Pennington, W. T. *J. Am. Chem. Soc.* **1983**, *105*, 6008.

(4) (a) Trsic, M.; Laidlaw, W. T.; Oakley, R. T. *Can. J. Chem.* **1982**, *60*, 2281. (b) Chivers, T.; Codding, P. W.; Laidlaw, W. G.; Liblong, S. W.; Oakley, R. T.; Trsic, M. *J. Am. Chem. Soc.* **1982**, *104*, 1282. (c) Laidlaw, W. G.; Trsic, M. *Inorg. Chem.* **1984**, *23*, 1981. (d) Bojes, J.; Chivers, T.; Laidlaw, W. G.; Trsic, M. *J. Am. Chem. Soc.* **1979**, *101*, 4517. Trsic, M.; Laidlaw, W. G. *Int. J. Quantum Chem.: Quantum Chem. Symp.* **1983**, *No. 17*, 367.

(5) (a) Waluk, J. W.; Michl, J. *Inorg. Chem.* **1982**, *21*, 556. (b) Waluk, J. W.; Michl, J. *Inorg. Chem.* **1981**, *20*, 963. (c) Waluk, J. W.; Chivers, T.; Oakley, R. T.; Michl, J. *Inorg. Chem.* **1982**, *21*, 832.

rings and benzenoid aromatics have never been attempted, in large part because the physical and chemical criteria used to assess aromaticity in carbocyclic systems (i.e. ring currents, resonance energies)⁶ have no experimentally observable counterparts in binary sulfur–nitrogen chemistry.

In an attempt to bridge the gap between sulfur–nitrogen and benzenoid chemistry we have directed our synthetic efforts toward the design of heterocyclic molecules that incorporate the chemical and electronic features of both conjugated thiazyl units and carbocyclic π -systems.^{7–11} Two molecules of particular interest in this context are the 12- π -electron 1,3,2,4-benzodithiadiazine⁹ (**1**) and the 14- π -electron 1,3,5,2,4-benzotrithiadiazepine^{11,12} (**2**).



Here we compare the structural features of these two molecules in the light of MNDO molecular orbital calculations on their ground state electronic structures. In addition we report the preparation and X-ray structural characterization of their two norbornadiene (NBD) adducts **3** and **4**. The electronic spectra, electrochemical behavior, and ¹H NMR shifts of **1** and **2** and the dissociation constants of their NBD adducts are discussed in relation to their aromatic/antiaromatic character.

Experimental Section

Starting Materials and General Procedures. (Trimethylsilyl)sulfonylamine,¹³ 1,2-bis(chlorothio)benzene,¹⁴ and sulfur bis[(trimethylsilyl)imide]¹⁵ were all prepared according to literature methods. *N*-(Trimethylsilyl)aniline (Petraich), sulfur dichloride (Aldrich), *n*-butyllithium (1.6 M) in hexane (Aldrich), norbornadiene (Aldrich), and trimethylsilyl chloride (Aldrich) were obtained commercially. With the exception of sulfur dichloride, which was distilled prior to use, all these reagents were used as received. The solvents methylene chloride and diethyl ether were dried by distillation from P₂O₅ and LiAlH₄, respectively, before use. All reactions were carried out under an atmosphere of nitrogen. Infrared spectra were recorded on Nujol mulls with the use of CsI cells and a Perkin-Elmer 1330 grating spectrophotometer. UV-visible spectra were recorded on a Cary 219 spectrophotometer. ¹H and ¹³C NMR spectra were recorded on a Bruker WH-400 spectrometer. Low-resolution mass spectra (EI) were measured on a VG 7070 EF spectrometer at 70 eV, samples being admitted through conventional inlet

systems. Elemental analyses were performed by MHW laboratories, Phoenix, AZ.

Electrochemical Measurements. Electrochemical oxidations of C₆H₄S₂N₂ and C₆H₄S₃N₂ were carried out in acetonitrile at a rotating platinum electrode with 0.1 M Et₄N⁺ClO₄⁻ as supporting electrolyte. Reductions were performed at a dropping-mercury electrode by using the same solvent and electrolyte. Half-wave potentials are quoted with reference to a saturated calomel electrode (SCE).

Preparation of PhNSNSiMe₃.¹⁶ A 1.6 M solution of *n*-butyllithium in hexane (46.0 mL, 73.6 mmol of *n*-BuLi) was added dropwise to a solution of Me₃SiNHPPh (12.2 g, 73 mmol) in 300 mL of diethyl ether and the resulting solution stirred at room temperature for 30 min. A solution of Me₃SiNSO (10.0 g, 74 mmol) in 30 mL of diethyl ether was then added and the resulting mixture stirred at room temperature overnight. The reaction was finally quenched by the addition of Me₃SiCl (8.0 g, 74 mmol) in 30 mL of diethyl ether. Filtration of the resulting mixture (to remove LiCl) and evaporation of the solvent gave a yellow oil, which was vacuum-distilled to yield PhNSNSiMe₃ (13.4 g, 64 mmol, 87%; bp 60–62 °C (0.01 torr)), which was identified by its ¹H NMR spectrum.¹⁷

Preparation of C₆H₄S₂N₂ (1**).** Equimolar solutions of PhNSNSiMe₃ (2.00 g, 9.52 mmol) and sulfur dichloride (0.98 g, 9.52 mmol) in 7.0 mL of CH₂Cl₂ were simultaneously injected (with a syringe pump) over a 7-h period into a stirred reservoir of 300 mL of CH₂Cl₂. The resulting dark green mixture was then filtered and the solvent removed from the filtrate in vacuo to leave a green-black paste. Heating this residue to 50 °C (0.01 torr) yielded a dark blue sublimate, which was collected on a -78 °C (acetone/dry ice) cold finger. The sublimate was further purified by repeated sublimation in vacuo and recrystallization from pentane to yield blue-black air-stable needles of C₆H₄S₂N₂ (0.525 g, 3.12 mmol, 33%; mp 48–50 °C). Anal. Calcd for C₆H₄S₂N₂: C, 42.86; H, 2.38; N, 16.67. Found: C, 43.12; H, 2.62; N, 16.56. Mass spectrum (EI, 70 eV), *m/e*: 168 (C₆H₄S₂N₂⁺, 100%), 154 (C₆H₄S₂N₂⁺, 12%), 136 (C₆H₄SN₂⁺, 50%), 122 (C₆H₄S⁺, 12%), 108 (C₆H₄N⁺, 12%). UV-visible (CH₂Cl₂), λ_{\max} , nm (log ϵ): 617 (2.7), 371 (3.0), 291 (4.3), 283 (4.3). Infrared (1600–250-cm⁻¹ region): 1435 (m), 1268 (vw), 1218 (s), 1158 (vw), 1091 (s), 1052 (m), 1027 (w), 943 (w), 791 (w), 759 (vs), 706 (w), 685 (w), 664 (w), 630 (m), 416 (w), 359 (m), 302 (w). ¹³C NMR (CDCl₃), δ : 138.8, 133.3, 130.6, 124.1, 123.8, 115.6.

Preparation of C₆H₄S₃N₂ (2**).** Equimolar solutions of 1,2-bis(chlorothio)benzene and Me₃SiNSNSiMe₃ (6.07 mmol in 9.0 mL of CH₂Cl₂) were injected simultaneously over a 9-h period with a syringe pump into a stirred reservoir of 300 mL of CH₂Cl₂. The resulting orange mixture was then filtered and the solvent removed from the filtrate in vacuo to yield an orange solid. Heating this residue at 60 °C (0.01 torr) yielded a yellow sublimate (collected on a water-cooled finger). The sublimate was further purified by column chromatography on Bio-Beads SX-8 using toluene as an eluting solvent. Finally, recrystallization from hot hexane afforded yellow air-stable needles of C₆H₄S₃N₂ (**2**) (0.497 g, 2.49 mmol, 41%; mp 78–80 °C). Anal. Calcd for C₆H₄S₃N₂: C, 35.98; H, 2.01; N, 13.99; S, 48.02. Found: C, 35.94; H, 2.14; N, 14.16; S, 47.81. Mass spectrum (EI, 70 eV), *m/e*: 200 (C₆H₄S₃N₂⁺, 79%), 154 (C₆H₂S₂N₂⁺, 100%), 108 (C₆H₄S⁺, 28%). UV-visible (CH₂Cl₂), λ_{\max} , nm (log ϵ): 384 (3.7), 347 (sh, 3.5), 294 (4.0), 256 (4.3). Infrared (1600–250-cm⁻¹ region): 1245 (s), 1178 (s), 1091 (w), 770 (w), 743 (s), 666 (s), 622 (w), 601 (m), 558 (w), 531 (m), 442 (m), 350 (m), 302 (m), 277 (m). ¹³C NMR (CDCl₃), δ : 147.0, 122.8, 121.7.

Preparation of C₆H₄S₂N₂·C₇H₈ (3**) and C₆H₄S₃N₂·C₇H₈ (**4**).** These adducts were both prepared by adding a large (~10-fold) excess of norbornadiene to a solution of **1** and **2** in ether. The adducts crystallized from solution in almost quantitative yield. C₆H₄S₂N₂·C₇H₈ (**3**) crystallizes as yellow platelets, dec pt >116 °C.¹⁸ Anal. Calcd for C₁₃H₁₂N₂S₂: C, 59.97; H, 4.65; N, 10.76. Found: C, 59.80; H, 4.53; N, 10.85. C₆H₄S₃N₂·C₇H₈ (**4**) crystallizes as yellow platelets, mp 78–81 °C. Anal. Calcd for C₁₃H₁₂N₂S₃: C, 53.39; H, 4.14; N, 9.58. Found: C, 53.29; H, 4.27; N, 9.73.

Dissociation Constants of **3 and **4**.** The dissociation constant between **3** and free **1** and norbornadiene was estimated by measuring the intensity

- (6) (a) Haddon, R. C. *J. Am. Chem. Soc.* **1979**, *101*, 1722. (b) Haigh, C. W.; Mallion, R. B. *Prog. Nucl. Magn. Reson. Spectrosc.* **1980**, *13*, 303.
- (7) Boeré, R. T.; Cordes, A. W.; Oakley, R. T. *J. Chem. Soc., Chem. Commun.* **1985**, 929.
- (8) (a) Cordes, A. W.; Hayes, P. J.; Josephy, P. D.; Koenig, H.; Oakley, R. T.; Pennington, W. T. *J. Chem. Soc., Chem. Commun.* **1984**, 1021. (b) Hayes, P. J.; Oakley, R. T.; Cordes, A. W.; Pennington, W. T. *J. Am. Chem. Soc.* **1985**, *107*, 1346.
- (9) Koenig, H.; Oakley, R. T. *J. Chem. Soc., Chem. Commun.* **1983**, 73.
- (10) Coddling, P. W.; Koenig, H.; Oakley, R. T. *Can. J. Chem.* **1983**, *61*, 1562.
- (11) We have independently prepared and structurally characterized **2**. We provide full details of our synthetic work but utilize the structural data provided in ref 12a for our structural comparisons of **1** and **2**.
- (12) (a) Morris, J. L.; Rees, C. W.; Rigg, D. J. *J. Chem. Soc., Chem. Commun.* **1985**, 55. (b) Daley, S. T. A. K.; Rees, C. W.; Williams, D. J. *J. Chem. Soc., Chem. Commun.* **1985**, 57.
- (13) (a) Scherer, O. J.; Wolmershäuser, G.; Jotter, R. Z. *Naturforsch., B: Anorg. Chem., Org. Chem.* **1982**, *37B*, 432. (b) Scherer, O. J.; Hornig, P. *Angew. Chem., Int. Ed. Engl.* **1966**, *5*, 729.
- (14) Feher, F.; Malcharek, F.; Glinka, K. Z. *Naturforsch., B: Anorg. Chem., Org. Chem., Biochem., Biol.* **1971**, *26B*, 67.
- (15) Scherer, O. J.; Weis, R. Z. *Naturforsch., B: Anorg. Chem., Org. Chem., Biochem., Biophys., Biol.* **1970**, *25B*, 1486.

(16) The preparation of this compound from the reaction of PhNSO and LiN(SiMe₃)₂¹⁷ affords a yield of 26%. The method described herein significantly improves the yield to 87%.

(17) Ruppert, I.; Bastian, V.; Appel, R. *Chem. Ber.* **1975**, *108*, 2329.

(18) The adduct **3** also crystallizes as yellow orthorhombic needles, space group *Pbcn*, *a* = 23.735 (4) Å, *b* = 9.130 (3) Å, *c* = 11.014 (5) Å, *V* = 2387 Å³, *Z* = 8. The molecular structure of the adduct is virtually identical with that reported here. There are two minor differences: the angles formed by the Si–C bonds between the heterocyclic rings and norbornadiene. The N(2)–S(2)–C(7) and C(1)–S(1)–C(12) angles are each 205°, or 12 standard deviations, greater than in the *Pbcn* form. This we ascribe to subtle differences in the packing forces of the two lattices.

Table I. Data for the Structure Determinations of 1, 3, and 4

	1	3	4
A. Crystal Data			
fw	168.2	260.4	294.2
cryst syst	monoclinic	orthorhombic	orthorhombic
space group	<i>Pc</i>	<i>Pbca</i>	<i>Pbca</i>
no. of refl in cell detn	25	25	25
<i>a</i> , Å	5.616 (1)	10.230 (3)	10.571 (2)
<i>b</i> , Å	3.896 (1)	19.922 (7)	11.914 (2)
<i>c</i> , Å	15.434 (3)	11.331 (6)	20.027 (3)
β , deg	102.23 (2)		
<i>V</i> , Å ³	330.0 (1)	2309	2522
<i>D</i> _{calcd} , g cm ⁻³	1.69	1.50	1.54
μ (Mo K α), cm ⁻¹	6.8	4.2	5.4
<i>Z</i>	2	8	8
size, mm	0.15 × 0.15 × 0.30	0.08 × 0.52 × 0.52	0.03 × 0.3 × 0.3
total decay, %	9.3	4.9	0.2
abs corr	none	0.87–0.94	0.77–0.97
B. Data Collection			
scan type	θ – 2θ	ω – θ	ω – 2θ
scan range (<i>a</i> + <i>b</i> tan θ), deg	1.05, 0.52	1.0, 0.35	1.0, 0.35
total no. of unique refl	788	3729	3672
no. of obsd. data (<i>I</i> > 3 σ (<i>I</i>))	634	1175	2034
2 θ range, deg	2–60	4–60	2–55
temp, °C	–115 (2)	22	22
C. Refinement			
no. of params refined	105	154	163
<i>R</i> ($\sum \Delta F / \sum F_o$)	0.040	0.044	0.040
<i>R</i> _w ($\sum w \Delta F ^2 / \sum w F_o ^2$) ^{1/2}	0.049	0.046	0.049
GOF ($\sum [w\Delta F]^2 / [N_o - N_v]$) ^{1/2}	1.36	1.41	1.21
refl/param ratio	6.0/1	7.6/1	12.5/1
max shift/error	0.03	0.001	0.01
final diff map max	0.3	0.24	0.27
<i>p</i> factor of counting statistics for weights	0.07	0.03	0.05

of the 617-nm band of **1** in solutions of **3** in chloroform (at 25 °C). The corresponding dissociation constant between **4** and **2** was more easily obtained from the relative intensities of free and complexed norbornadiene in solutions of **4** in CDCl₃ (at 25 °C) by using ¹H NMR spectroscopy. The reported values of *K*_{diss} are averages derived from a range of initial concentrations of **3** and **4** spread over 2 orders of magnitude.

X-ray Measurements. Crystals of **1**, **3**, and **4** (Table IA) were mounted on glass fibers with epoxy. X-ray data were collected by using an Enraf Nonius CAD4 diffractometer employing graphite-monochromated Mo K α ($\lambda = 0.71073$ Å) radiation at –115 °C for **1** and at ambient temperature for **3** and **4**. Data collection parameters are listed in Table IB.

The structures were solved by direct methods (MULTAN11/82)¹⁹ and refined (Table IC) by full-matrix least-squares analyses based on ($|F_o| - |F_c|$)². Hydrogen atom positions and isotropic temperature factors for the hydrogens were refined in **1**. Hydrogen atom positions were constrained to idealized positions in **3** and **4**. Weighting schemes gave no systematic variation in *F*/ σ (*F*) as a function of *F* or sin θ . No secondary extinction corrections were made. Neutral-atom scattering factors^{20a} were corrected for real and imaginary anomalous dispersion.^{20b} The computer programs used were those provided by the Enraf Nonius structure determination package. Non-hydrogen atom coordinates for **1**, **3**, and **4** are given in Table II, and selected bond distance and angle data are provided in Table III. Tables containing anisotropic thermal parameters for the three structures have been deposited as supplementary material.

Theoretical Method and Models. The MNDO (modified neglect of diatomic overlap) method²¹ has been used extensively for the study of the electronic structures of sulfur nitride derivatives.³ In this study calculations involving full geometry optimization, within *C_s* symmetry for **1**

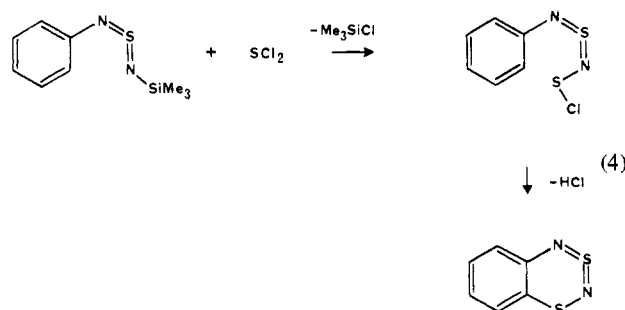
and *C_{2v}* symmetry for **2**, were performed by using the MOPAC program.^{21b} Bond orders and charge densities refer to the elements of the Coulson density matrix.

Results and Discussion

Preparation of 1–4. The use of sulfur bis[(trimethylsilyl)imide], Me₃SiNSNSiMe₃, as a coupling reagent in the preparation of open-chain, cyclic, and cage sulfur nitride derivatives is a well-established synthetic method.^{13,22} In the case of monosilylated sulfur diimides, e.g. *t*-BuNSNSiMe₃, similar reactivity patterns are observed, and α,ω -dialkyl S_xN_{x+} chains have been prepared in high yield (eq 3).¹⁷ However, while attempting to extend such



reactions to allow the preparation of aryl-substituted chains, we discovered that the reaction of PhNSNSiMe₃ with SCl₂ did not proceed in the anticipated manner. Instead, electrophilic attack of the sulfonyl chloride residue of the supposed intermediate at the ortho position of the phenyl ring occurred, resulting in the formation of the novel bicyclic ring system 1,3,2,4-benzodithiadiazine **1** (eq 4). In our initial investigation of this reaction



(19) Main, P. MULTAN/82, a system of computer programs for the automatic solution of crystal structures from X-ray diffraction data, University of York, England.

(20) (a) Cromer, D. T.; Weber, J. T. "International Tables for X-ray Crystallography"; Kynoch Press: Birmingham, England, 1974; Vol. IV, Table 2.2B. (b) Cromer, D. T. "International Tables for X-ray Crystallography"; Kynoch Press: Birmingham, England, 1974; Vol. IV, Table 2.3.1.

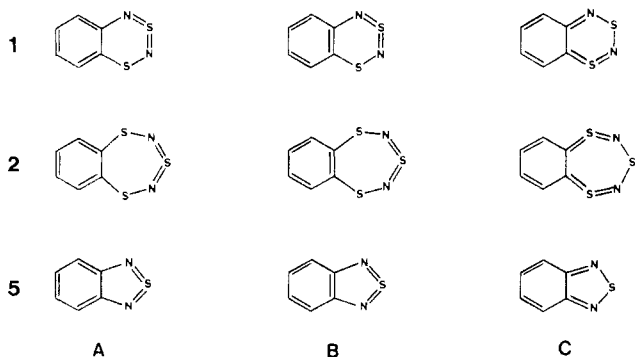
(21) (a) Dewar, M. J. S.; Thiel, W. J. *Am. Chem. Soc.* **1977**, *99*, 4899. (b) *QCPE* **1984**, No. 455 (MOPAC).

(22) (a) Lidy, W.; Sundermeyer, W.; Verbeek, W. Z. *Anorg. Allg. Chem.* **1984**, *406*, 228. (b) Kuyper, J.; Street, G. G. *J. Am. Chem. Soc.* **1977**, *99*, 7848. (c) Chivers, T.; Oakley, R. T.; Pieters, R.; Richardson, J. F. *Can. J. Chem.* **1985**, *63*, 929.

Table II. Non-Hydrogen Atom Coordinates and B_{eq} Values^a for **1**, **3**, and **4**

atom	x	y	z	$B_{eq}, \text{\AA}^2$
Compound 1				
S(1)	1.0701 (2)	0.0559 (3)	1.02393 (7)	1.71 (2)
S(2)	0.625	0.4272 (3)	1.001	1.79 (2)
N(1)	0.8100 (6)	0.217 (1)	0.9613 (2)	1.96 (7)
N(2)	0.6744 (6)	0.496 (1)	1.1017 (3)	1.68 (7)
C(1)	1.0746 (6)	0.192 (1)	1.1354 (2)	1.25 (7)
C(2)	1.2791 (7)	0.092 (1)	1.1975 (3)	1.50 (7)
C(3)	1.2987 (7)	0.175 (1)	1.2872 (3)	1.85 (8)
C(4)	1.1129 (7)	0.350 (1)	1.3138 (3)	1.73 (7)
C(5)	0.9062 (7)	0.450 (1)	1.2501 (3)	1.54 (8)
C(6)	0.8868 (7)	0.373 (1)	1.1611 (3)	1.35 (7)
Compound 3				
S(1)	0.3099 (1)	0.07089 (5)	0.2543 (1)	4.09 (2)
S(2)	0.1364 (1)	0.05330 (6)	0.0882 (1)	5.19 (3)
N(1)	0.1552 (3)	0.0577 (2)	0.2341 (3)	5.34 (9)
N(2)	0.1743 (4)	0.1218 (2)	0.0241 (3)	5.57 (9)
C(1)	0.3458 (4)	0.1438 (2)	0.1747 (3)	4.01 (9)
C(2)	0.4395 (5)	0.1869 (2)	0.2201 (4)	5.6 (1)
C(3)	0.4689 (5)	0.2444 (3)	0.1627 (5)	7.7 (2)
C(4)	0.4048 (6)	0.2595 (2)	0.0611 (5)	8.3 (2)
C(5)	0.3094 (6)	0.2196 (2)	0.0172 (5)	7.0 (1)
C(6)	0.2744 (4)	0.1597 (2)	0.0724 (4)	4.8 (1)
C(7)	0.2740 (3)	-0.0033 (2)	0.0595 (3)	3.34 (8)
C(8)	0.2427 (4)	-0.0785 (2)	0.0727 (4)	4.06 (9)
C(9)	0.3646 (4)	-0.1136 (2)	0.0335 (4)	4.3 (1)
C(10)	0.4533 (4)	-0.1040 (2)	0.1152 (4)	3.97 (9)
C(11)	0.3931 (4)	-0.0623 (2)	0.2115 (3)	3.57 (9)
C(12)	0.3787 (3)	0.0079 (2)	0.1554 (3)	2.93 (8)
C(13)	0.2534 (4)	-0.0892 (2)	0.2062 (4)	4.4 (1)
Compound 4				
S(1)	0.43140 (3)	0.24805 (6)	0.21623 (7)	2.57 (1)
S(2)	0.46036 (4)	0.09589 (6)	0.40001 (6)	2.98 (1)
S(3)	0.35438 (4)	-0.01702 (6)	0.27303 (8)	3.36 (1)
N(1)	0.4449 (1)	0.2288 (2)	0.3657 (2)	3.10 (5)
N(2)	0.3938 (1)	0.0214 (2)	0.4069 (20)	3.25 (5)
C(1)	0.3513 (1)	0.2022 (2)	0.1658 (3)	2.62 (5)
C(2)	0.3200 (2)	0.2802 (3)	0.0869 (3)	3.53 (6)
C(3)	0.2604 (2)	0.2552 (3)	0.0281 (3)	4.58 (7)
C(4)	0.2314 (2)	0.1524 (3)	0.0497 (3)	4.55 (8)
C(5)	0.2604 (2)	0.0762 (3)	0.1304 (3)	3.79 (7)
C(6)	0.3212 (1)	0.0979 (2)	0.1890 (3)	2.80 (5)
C(7)	0.5053 (1)	0.0579 (2)	0.2531 (3)	2.50 (5)
C(8)	0.5827 (1)	0.0704 (2)	0.2664 (3)	2.99 (5)
C(9)	0.6102 (1)	0.0270 (3)	0.1429 (3)	3.39 (6)
C(10)	0.5953 (2)	0.0998 (3)	0.0540 (3)	3.32 (6)
C(11)	0.5573 (1)	0.1952 (2)	0.1152 (3)	2.66 (5)
C(12)	0.4882 (1)	0.1424 (2)	0.1477 (2)	2.28 (5)
C(13)	0.5921 (1)	0.1968 (2)	0.2453 (3)	3.00 (5)

^a Anisotropically refined atoms are given in the form of the isotropic equivalent thermal parameter defined as $\frac{4}{3}[a^2\beta_{11} + b^2\beta_{22} + c^2\beta_{33} + ab(\cos \gamma)\beta_{12} + ac(\cos \beta)\beta_{13} + bc(\cos \alpha)\beta_{23}]$.

Chart I

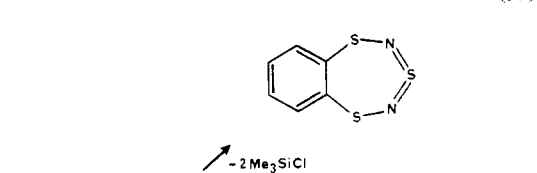
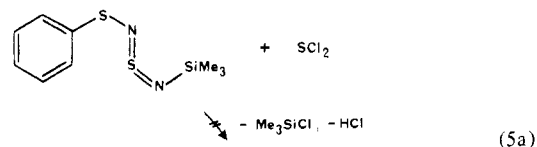
we employed standard addition methods to mix the reagents, and rather low yields (<12%) were obtained. We have since improved the yield significantly (to 33%) by the use of high-dilution addition techniques, which tend to favor the intramolecular cyclization over

Table III. Selected Bond and Angle Data in **1**, **3**, and **4**

atom 1	atom 2	distance, \AA			
		1	3	4	
S(1)	N(1)	1.693 (3)	1.621 (3)	1.621 (2)	
S(1)	C(1)	1.796 (4)	1.749 (4)	1.778 (3)	
S(1)	C(12)		1.824 (3)	1.845 (2)	
S(2)	N(1)	1.547 (4)	1.666 (3)	1.654 (2)	
S(2)	N(2)	1.544 (4)	1.594 (4)	1.603 (2)	
S(2)	C(7)		1.834 (3)	1.851 (3)	
S(3)	N(2)			1.685 (2)	
S(3)	C(6)			1.762 (3)	
N(2)	C(6)	1.423 (5)	1.385 (5)		
C(1)	C(2)	1.387 (5)	1.386 (5)	1.398 (4)	
C(1)	C(6)	1.394 (5)	1.406 (5)	1.403 (4)	
C(2)	C(3)	1.403 (6)	1.350 (6)	1.379 (4)	
C(3)	C(4)	1.381 (6)	1.358 (7)	1.375 (5)	
C(4)	C(5)	1.407 (5)	1.354 (7)	1.375 (5)	
C(5)	C(6)	1.387 (6)	1.393 (6)	1.392 (4)	
C(7)	C(12)		1.542 (4)	1.541 (3)	
		angle, deg			
atom 1	atom 2	atom 3	1	3	4
N(1)	S(1)	C(1)	105.8 (2)	105.5 (2)	113.6 (1)
N(1)	S(1)	C(12)		100.3 (2)	100.6 (1)
C(1)	S(1)	C(12)		100.1 (2)	103.2 (1)
N(1)	S(2)	N(2)	119.9 (2)	112.3 (2)	112.6 (1)
N(1)	S(2)	C(7)		96.9 (2)	98.1 (1)
N(2)	S(2)	C(7)		105.0 (2)	107.9 (1)
N(2)	S(3)	C(6)			112.9 (1)
S(1)	N(1)	S(2)	122.7 (2)	105.2 (2)	112.4 (1)
S(2)	N(2)	S(3)			120.1 (1)
S(2)	N(2)	C(6)	122.5 (3)	117.8 (3)	
S(1)	C(1)	C(2)	114.9 (3)	117.9 (3)	112.3 (2)
S(1)	C(1)	C(6)	124.3 (3)	120.2 (3)	127.4 (2)
C(2)	C(1)	C(6)	120.8 (3)	121.7 (4)	120.1 (3)
C(1)	C(2)	C(3)	119.8 (4)	120.0 (5)	120.9 (3)
C(2)	C(3)	C(4)	120.1 (3)	119.2 (5)	118.9 (3)
C(3)	C(4)	C(5)	119.5 (4)	122.0 (6)	120.9 (3)
C(4)	C(5)	C(6)	120.9 (4)	121.5 (5)	121.6 (3)
S(3)	C(6)	C(1)			127.9 (2)
N(2)	C(6)	C(1)	124.6 (3)	125.9 (4)	
S(3)	C(6)	C(5)			114.2 (2)
N(2)	C(6)	C(5)	116.4 (4)	118.6 (4)	
C(1)	C(6)	C(5)	119.0 (3)	115.4 (5)	117.5 (3)

bimolecular processes. 1,3,2,4-Benzodithiadiazine is a deep blue volatile crystalline solid (mp 48–50 °C) with an odor similar to that of naphthalene. It is extremely soluble in all common organic solvents and insoluble in water. It slowly hydrolyzes in moist air or on prolonged contact with water. It is thermally stable and can be recovered unchanged after being heated at reflux in boiling toluene for 24 h.

We have also explored the reaction of PhSNSNSiMe₃ (prepared from Me₃SiNSNSiMe₃ and phenylsulfenyl chloride)^{22b} with sulfur dichloride, the intention being to generate the 1,3,5,2,4-benzotrithiadiazepine system via an annelation sequence (eq 5a)



analogous to that described above. However, we were unable to isolate any cyclized product; only PhSNSNSPh and some [PhSNSNSNSPh]⁺Cl⁻ were obtained.^{22b} Presumably, the longer

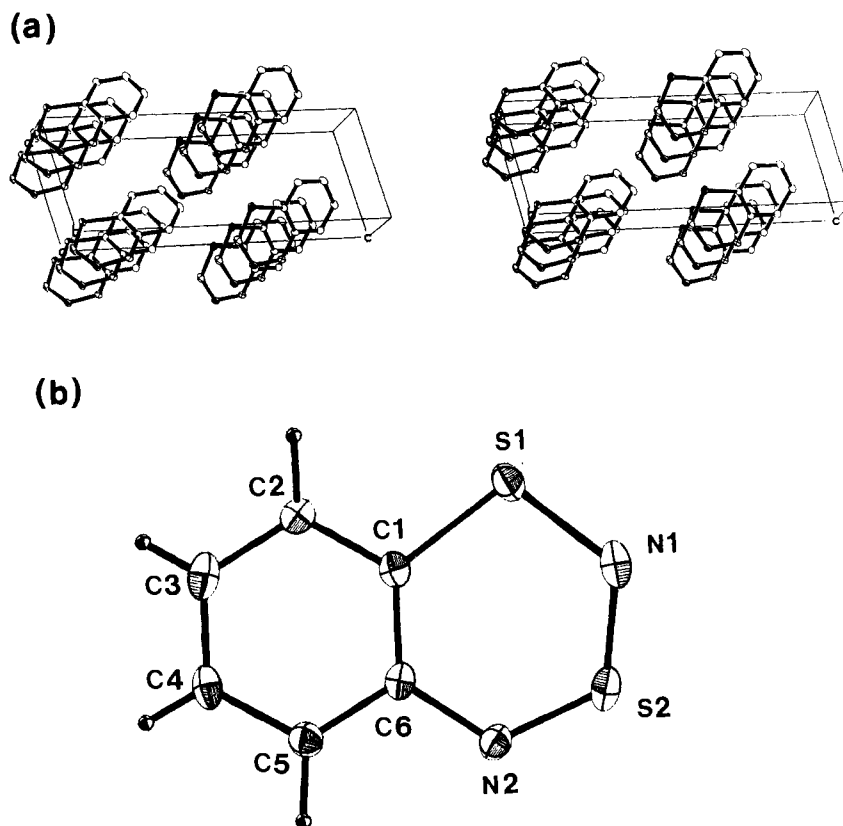


Figure 1. (a) Crystal packing and (b) ORTEP view (50% probability ellipsoids) of a single molecule of $C_6H_4S_2N_2$ (**1**).

PhSNSNSiMe₃ chain is too conformationally rigid (cf. RSNSS and RNSO derivatives)^{22c} to allow an electrophilic attack of the sulfonyl chloride intermediate on the aromatic ring. Eventually, we¹¹ and others¹² found a relatively efficient route to the desired product via the coupling of Me₃SiSNSiMe₃ with 1,2-bis(chlorothio)benzene (eq 5b). Like **1**, **2** is extremely stable, with respect to both thermolysis and hydrolysis. This thermal stability is in contrast to the behavior of open-chain RSNSNSR derivatives²³ and S₄N₂,^{4b} which decompose on heating.

The two adducts **3** and **4** are easily obtained by the addition of norbornadiene to solutions of **1** and **2** in diethyl ether (eq 1 and 2). The driving force for the reactions is largely the lattice energy of the adducts; if dissolved in methylene chloride or chloroform, both adducts partially dissociate into their separate components. For example, solutions of **3** in organic media, e.g. chloroform or methylene chloride, develop a pale green color on standing due to the formation of **1** and free norbornadiene. K_{diss} for this reaction, as determined spectrophotometrically, is 5×10^{-6} M. By contrast, **4** dissociates to a much larger degree. Because the colors of **2** and **4** are quite similar, the change is not visibly noticeable, but it is easily monitored by ¹H NMR spectroscopy. K_{diss} for this reaction is 6×10^{-2} M. The relevance of these K_{diss} values to the aromatic characters of **1** and **2** is discussed below.

Crystal Structure of 1. Compound **1** crystallizes in the non-centrosymmetric space group *Pc* with *x* and *z* axes polar. The long axis of the molecule has a substantial component along the *z* axis, with the S–N portion of all molecules pointing toward $-z$; also, all molecules are oriented such that the N(1)–S(2) vector has a major component in the $+x$ direction. The crystal structure of **1** (Figure 1a) consists of columns of parallel molecules formed by unit translations along the *b* axis. The uniform interplanar separation of 3.29 Å is less than that found in 1,3-diazanaphthalene (3.46–3.62 Å),²⁴ naphtho[1,8-*cd*:4,5-*c'd'*]bis[1,2,6]thiadiazine (3.40 Å),²⁵ and graphite (3.35–3.37 Å)²⁶ and is nearly equivalent

to that observed in donor–acceptor π -complexes such as skatole–trinitrobenzene (3.30 Å),²⁷ anthracene–trinitrobenzene (3.28 Å),²⁸ and pyrene–pyromellitic dianhydride (3.30–3.33 Å).²⁹ The molecules are inclined at an angle of 57.5° to the *b* axis, resulting in an overlap pattern similar to that observed in graphite,³⁰ in which each six-membered ring has centered above and below it an atom from a neighboring molecule in the stack. This mode of packing is the reverse of the head-to-tail arrangement found for **2**.¹²

Comparison of the Molecular Structures of 1 and 2. An ORTEP drawing of **1** is provided in Figure 1b. The molecule is essentially planar, to within 0.04 Å. We begin the discussion of the structural parameters of this molecule in a valence-bond context, by comparing the bond lengths in **1** with those observed in **2**¹² and the related 2,1,3-benzothiadiazole (**5**).³¹ The relevant data are compiled in Table IV. Simple inspection of the variations observed in the three structures reveals a marked difference in their electronic structures. While **5** exhibits long N–S–N bonds typical of the quinoid representation C (Chart 1), both **1** and **2** possess more compact N–S–N units, which are suggestive of the diimide formulations A and B. The quinoid vs. diimide demarcation is also clearly demonstrated by the variations in the C–C distances within the benzene ring, the relative lengths of the C_a–C_b and C_b–C_c bonds (Table IV) in particular providing a useful criterion for the relative contributions of the quinoid C and diimide A and B structures. On this basis one can additionally conclude that, at least in relation to **1**, there is some involvement of the quinoid

(23) Golloch, A.; Kuss, M. *Z. Naturforsch., B: Anorg. Chem., Org. Chem., Biochem., Biophys., Biol.* **1972**, *27B*, 1280.
 (24) Huiszoon, C. *Acta Crystallogr., Sect. B: Struct. Crystallogr. Cryst. Chem.* **1976**, *B32*, 998.

(25) Gieren, A.; Lamm, V.; Haddon, R. C.; Kaplan, M. L. *J. Am. Chem. Soc.* **1979**, *101*, 7277.
 (26) Laves, F.; Baskin, Y. *Z. Kristallogr., Kristallgeom., Kristallphys., Kristallchem.* **1956**, *107*, 337.
 (27) Hanson, A. W. *Acta Crystallogr.* **1964**, *17*, 559.
 (28) Brown, D.; Wallwork, S. C.; Wilson, A. *Acta Crystallogr.* **1964**, *17*, 168.
 (29) Herbstein, F. H.; Snyman, J. A. *Philos. Trans. R. Soc. London, A* **1969**, *No. 264*, 635.
 (30) Reynolds, W. N. "Physical Properties of Graphite"; Elsevier: Amsterdam, 1968.
 (31) Luzzati, V. *Acta Crystallogr.* **1951**, *4*, 193. The structural data should be viewed with caution ($R = 0.215$).

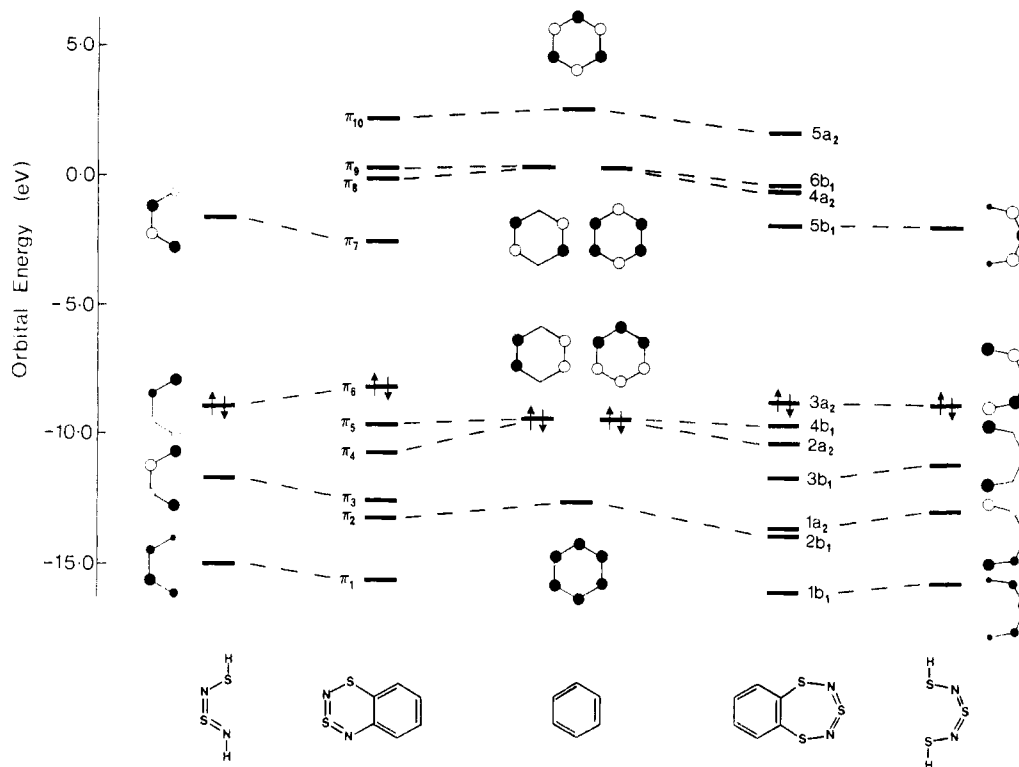


Figure 2. MNDO π molecular orbital energies of $C_6H_4S_2N_2$ (**1**), benzene, and $C_6H_4S_3N_2$ (**2**).

Table IV. Experimental Bond Lengths (Å) and Calculated (MNDO) π -Bond Orders in Selected Compounds^a

	1	2 ^b	5 ^c
A. Bond Lengths			
C _a -C _b	1.387 (N), 1.387 (S) ^d	1.421	1.46
C _b -C _c	1.407 (N), 1.403 (S) ^d	1.349	1.29
C _c -C _{c'}	1.381	1.396	1.46
C _a -C _{a'}	1.394	1.387	1.41
C-S	1.796	1.731	
C-N	1.423		1.34
N-S(C)	1.693	1.609	
S-N(C)	1.544		1.60
N-S-N (av)	1.546	1.538	1.60
B. π -Bond Orders			
C _a -C _b	0.711 (S), 0.659 (N) ^d	0.566	0.309
C _b -C _c	0.616 (S), 0.634 (N) ^d	0.747	0.901
C _c -C _{c'}	0.697	0.683	0.349
C _a -C _{a'}	0.569	0.578	0.952
C-S	0.0916	0.257	
C-N	0.0362		0.831
N-S(C)	0.0224	0.262	
S-N(C)	0.575		0.379
N-S-N (av)	0.637	0.606	0.379

^a Carbon atoms lettered alphabetically from the quaternary carbons.

^b Reference 12. ^c Reference 31. ^d Two chemically distinct values.

structure for **2**. The shorter C-S, N-S(C), and C_b-C_c bonds in **2** all illustrate this point. We also note the similarity in the bond lengths observed in **2** and the trithiadiazepine itself;¹² as in **2** the C-S and S-N distances in the latter are shortened relative to those found in RSNSNR (R = *p*-chlorophenyl)³² (average C-S and S-N(C) distances are 1.747 and 1.660 Å, respectively), in which cyclic conjugation is absent.

A series of MNDO molecular orbital calculations on **1**, **2**, and **5**³³ reveal overall π -bond order variations (see Table IVB) that provide a satisfying correlation with the experimental bond dis-

tances. Thus, the bond orders calculated for the N-S-N (average value), C_b-C_c, C-S, and N-S(C) linkages in the three molecules all conform to the overall conclusions of the structural work, namely the importance of the quinoid structure for **5**, the diimide formulation for **1**, and the somewhat intermediate situation for **2**.

The importance of the diimide formulations A and B for **1** can be interpreted in a molecular orbital context as reflecting a relatively weak interaction between the two "halves" of the molecule. A cursory examination of the (MNDO) π molecular orbitals of **1** confirms this idea. The molecule is indeed best described as two weakly coupled subunits, i.e. a benzene nucleus and an NSNS fragment. The situation is reminiscent of the S₄N₂ molecule, in which the π -manifold resembles two loosely connected pseudo-allylic (SSS and NSN) units.^{4b} To further illustrate this idea, we provide in Figure 2 an approximate correlation diagram for the π orbitals (MNDO) of **1** with those of benzene and a hypothetical HSNSNH fragment. Analysis of the individual π -distributions in **1** and in the two fragment molecules indicates that the occupied orbitals π_2 and π_4 and the virtual orbitals $\pi_{8,9,10}$ can all be designated as benzene-like. Likewise π_1 and π_7 clearly resemble, both energetically and spatially, the lowest and highest occupied orbitals of HSNSNH. The correspondence is less than perfect for π_3 and π_6 ; the former is strongly bonding over the N-C and N-S(C) linkages while the latter is antibonding, hence the rather weak bonds in these regions of the molecule.

A similar "molecules-within-molecules" approach can be attempted for **2**, but as expected from the structural analysis, which indicated more conjugation with the benzene nucleus than in **1**, the result is less satisfactory. For the virtual orbitals the correlations indicated in Figure 2 are fairly unequivocal, as they are for the occupied levels 1b₁, 1a₂, 2a₂, and 3a₂. However, in the 2b₁, 3b₁, and 4b₁ orbitals considerable mixing is evident. The first two orbitals contribute a net bonding interaction over the C-S linkages, while the last offsets the effect. The net result of the many orbital changes, but principally the redistribution of the π -HOMO of HSNSNSH, is a strengthening of the N-S(C) bonds in **2** relative to the N-S(H) bonds in HSNSNSH and a strengthening of the C-S bonds relative to that found in **1**.

The molecular orbital distributions of **1** and **2** thus reflect the same conclusions reached from the structural analysis, namely

(32) Olsen, F. P.; Barrick, J. C. *Inorg. Chem.* **1973**, *12*, 1353.

(33) From a calculation performed with full geometry optimization within C_{2v} symmetry.

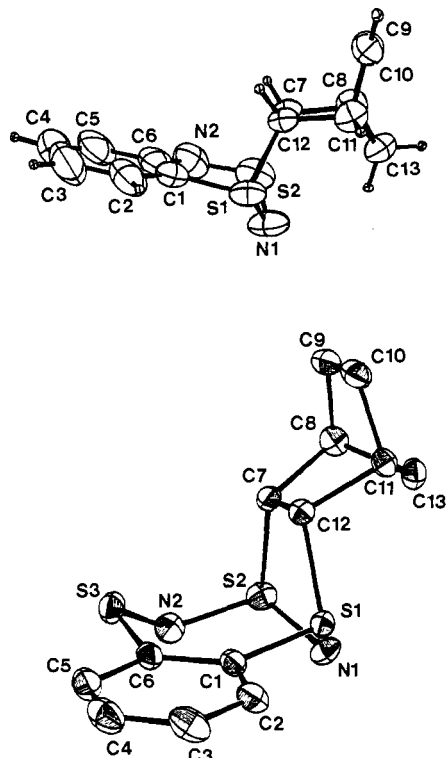


Figure 3. ORTEP drawings (50% probability ellipsoids) of (top) $C_6H_4S_2N_2C_7H_8$ (3) and (bottom) $C_6H_4S_3N_2C_7H_8$ (4).

Table V. Frontier Orbital (MNDO) Energies (eV) and Half-Wave Potentials (V vs. SCE) in Selected Compounds

compd	E_{HOMO}	E_{LUMO}	$E_{1/2}^{ox}$	$E_{1/2}^{red}$
1	-8.215	-2.286	+1.17	-0.57, -1.55
2	-8.501	-1.736	+1.36	-0.83
5 ^a	-9.616	-1.407	+2.2	-1.51, -2.5

^a Reference 36.

the weak coupling of the NSNS and C_6 units in **1** and the somewhat greater but still not uniform orbital mixing of the SNSNS and C_6 components of **2**.

Molecular Structures of 3 and 4. ORTEP drawings of **3** and **4** are given in Figure 3. The regio- and stereochemistry of adduct formation between **1**, **2** and norbornadiene is as observed elsewhere;³⁴ the olefin π -bond adds across two sulfur atoms in a 1,3-fashion. Reciprocally, the thiazyl heterocycle adds to the exo side of the norbornadiene molecule.³⁵ In both cases adduct formation causes a distortion from planarity for the thiazyl units. In **3** only N(1) undergoes a significant displacement, while in **4** the seven-atom $C_2N_2S_3$ ring folds into a pseudochair conformation. In **3** the S-N bond lengths all become more uniform (some contract while others elongate), whereas in **4** there is an irregular lengthening of all the S-N linkages. In relation to the above quinoid/diimide arguments, the complexation of norbornadiene to **1** induces some quinoid character to the structure; the C(2)-C(3) and C(4)-C(5) bonds are shortened by 0.05 Å. By contrast, the diimide form seems to be more pronounced in **4** than in **2**, the C(2)-C(3) and C(4)-C(5) distances being slightly longer.

Electrochemistry and Electronic Spectra of 1 and 2. The absolute energies of the virtual orbitals listed in Table V have little meaning by themselves. However, when taken together, the relative energies of the HOMO's and LUMO's of **1**, **2**, **5**, and benzene provide a reasonable model for correlating a variety of data. For example the somewhat higher E_{HOMO} values for **1** and **2** in comparison to those in **5** and benzene are consistent with their

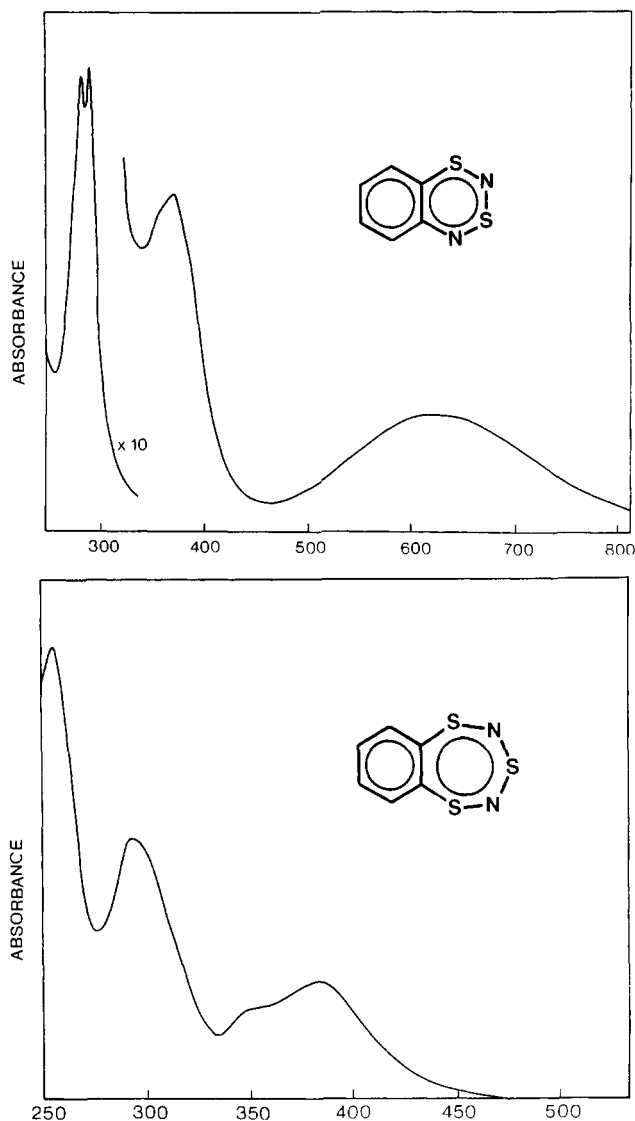
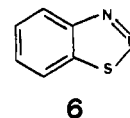


Figure 4. UV-visible spectra of (top) $C_6H_4S_2N_2$ (1) and (bottom) $C_6H_4S_3N_2$ (2).

relatively low oxidation potentials. Likewise, the low reduction potentials of **1** and **2**, particularly that of the former, parallel the trends in calculated LUMO energies. Indeed, in spite of their being "electron-rich" π -systems, both **1** and **2** are remarkably susceptible to reduction. They are both more easily reduced than either the 2,1,3-benzothiadiazole **5** or the corresponding 1,2,3-derivative **6** ($E_{1/2}^{red} = -1.64$ V).³⁶ In fact, **1** is as good an oxidant



as quinone ($E_{1/2}^{red} = -0.51$ V).³⁷ All these features reflect the combined influence of the high electronegativities of sulfur and nitrogen in generating extremely high electron affinities for the molecules. In binary sulfur nitrides, e.g. S_4N_4 ($E_{1/2}^{red} = -0.9$ V), similar effects are found.³⁸ Observations like these have prompted Fukui and co-workers to suggest the potential of binary sulfur nitrides in charge-transfer applications.³⁹ The present results

(34) See for example: Liblong, S. W.; Oakley, R. T.; Cordes, A. W.; Noble, M. C. *Can. J. Chem.* **1983**, *61*, 2062.

(35) Rondan, N. A.; Paddon-Row, M. N.; Caramella, P.; Houk, K. N. *J. Am. Chem. Soc.* **1981**, *103*, 2436.

(36) Atherton, N. M.; Ockwell, J. N.; Dietz, R. *J. Chem. Soc. A* **1967**, 771.

(37) Peover, M. E. *J. Chem. Soc.* **1962**, 4540.

(38) (a) Hojo, M. *Bull. Chem. Soc. Jpn.* **1980**, *53*, 2856. (b) Tweh, J. W.; Turner, A. G. *Inorg. Chim. Acta* **1981**, *48*, 73. (c) Chivers, T.; Hojo, M. *Inorg. Chem.* **1984**, *23*, 1526.

(39) Tanaka, K.; Yanabe, T.; Tachibana, A.; Kato, H.; Fukui, K. *J. Phys. Chem.* **1978**, *82*, 2121.

Table VI. ^1H Chemical Shifts (ppm) and Coupling Constants (Hz) of Aromatic Protons in Compounds 1–6^a

compd	δ_1, δ_4	δ_2, δ_3	$J_{1,2}$	$J_{1,3}$	$J_{2,3}$	$J_{2,4}$	$J_{3,4}$	$J_{1,4}$
1	5.90	6.78	8.14	0.9	8.2	1.4	7.8	0.2
	5.78	6.62						
2	7.26	7.74	9.0	0.8	6.7	0.8	9.0	0.4
3	6.85	7.18	8.0	1.6	6.9	1.1	8.4	0.0
	6.67	6.60						
4	7.86	7.31	8.0	1.3	6.7	1.2	7.4	0.0
5	7.966	7.531	8.53	1.15	6.66	1.15	6.66	0.89
6	8.610	7.614	8.35	1.04	7.05	1.00	7.88	0.78
	8.080	7.661						

^a Protons numbered sequentially around the perimeter.

augur well for the use of planar thiazyl heterocycles in such materials.

The electronic spectra of **1** and **2** are illustrated in Figure 4. We refrain at this time from a full analysis of these spectra but tentatively assign the lowest energy ($\lambda_{\text{max}} = 617 \text{ nm}$) absorption in **1** to a $\pi_6(\text{HOMO})-\pi_7(\text{LUMO})$ excitation. Similarly, we assign the lowest energy absorption band ($\lambda_{\text{max}} = 384 \text{ nm}$) in **2** to a $3a_2(\text{HOMO})-5b_1(\text{LUMO})$ excitation. While the calculated (MNDO) HOMO-LUMO gaps cannot be used in a direct comparison with observed transition energies, the trends in the observed and calculated energy gaps show a satisfying correspondence.

^1H NMR Spectra. The proton chemical shift and coupling constant data for **1**–**4** are listed in Table VI along with the analogous data for the related benzothiadiazoles **5** and **6**. The spectrum of **2** consists of a straightforward AA'XX' pattern, while that of **1** (see Figure 5) is complicated by the absence of a twofold axis. In both cases spectral parameters were confirmed by computer simulation. Even so, the absolute distinction between the 1- and 4- and the 2- and 3-positions in **1** remains unestablished. However, this particular point is not critical to our present discussion.

The interpretation of ^1H chemical shifts in carbocyclic π -systems in terms of aromatic character holds much appeal.^{40–42} The same concepts are no less applicable to the present heterocyclic systems. Thus, the marked difference between the 1,4-resonances of **6** (8.61 and 8.08 ppm)^{43,44} and **1** (5.50 and 5.70 ppm) reflect an intrinsic antiaromatic character for the latter. That the 2,3-protons of **1** undergo a relatively minor upfield shift between **6** and **1** can be interpreted, in a quantum-mechanical context, in terms of the excited state that dominates the paramagnetic shielding term. Our tentative assignment of the low-energy transition in **1** as a $\pi_6 \rightarrow \pi_7$ process, i.e. between orbitals localized over the NSNS fragment, would imply a greater paramagnetic shielding effect for the proximal 1,4-protons. By contrast, the 2,3-protons, which are more remote from the NSNS chromophore, should remain relatively unperturbed.

The chemical shift data for the adducts provide additional support for the above argument. In particular we draw attention to the resonances of the 1,4-protons in **3** (see Figure 5). Complexation of norbornadiene destroys the chromophore responsible for the paramagnetic shift, and the 1,4-proton signals return to a chemical shift range more in keeping with an aromatic compound.

The coupling constants in Table VI are also of interest. The relative values of such coupling constants between protons on adjacent carbons have often been used as a measure of the carbon-carbon bond order⁴⁵ and hence the degree of double-bond fixation in a molecule. The relative values of $J_{1,2}$ (also $J_{3,4}$) and

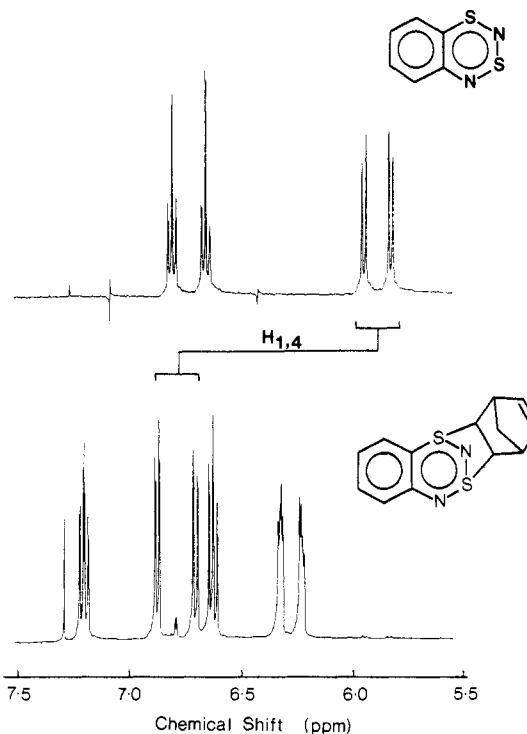


Figure 5. Aromatic region of ^1H NMR spectra of $\text{C}_6\text{H}_4\text{S}_2\text{N}_2$ and $\text{C}_6\text{H}_4\text{S}_2\text{N}_2 \cdot \text{C}_7\text{H}_8$.

$J_{2,3}$ should therefore provide an indication of the importance of the quinoid resonance formulation in the various molecules under consideration. The relatively large $J_{1,2}$ values in **5** and small $J_{1,2}$ and $J_{3,4}$ values in **6** illustrate the effect.^{43,44} The corresponding data for **1** and **2** can also be used quite convincingly to substantiate our previous conclusions regarding the diimide/quinoid balance. Thus, the low $J_{1,2}$ (and $J_{3,4}$) to $J_{2,3}$ ratios in **1** are consistent with a lack of bond localization in the benzene ring of **1**; the higher ratios observed in **2** indicate a greater localization into the quinoid structure. The quinoid/diimide balance in **3** and **4** can be assessed by using similar reasoning. In agreement with the structural results, some quinoid character seems to be introduced into **3** (compare the $J_{1,2}/J_{2,3}$ ratios in **1** and **3**), while in **4** the quinoid contribution appears to be reduced relative to that in **2**.

Conclusions

Aromaticity means different things to different people.⁴⁶ Consequently, the many observables that have been invoked to act as criteria for defining the concept of aromaticity do not always form a self-consistent set. Nonetheless, the existence of the concept has always provided a stimulus for the development of chemical ideas. While the rapid growth in binary sulfur nitride chemistry has been accompanied by an equal growth in theoretical interest, the relevance of the term aromaticity has never been properly considered. The two molecules **1** and **2** are unique in at least

(40) Benazzi, R.; Lazaretti, P.; Taddel, F. *Mol. Phys.* **1973**, *26*, 41.
 (41) (a) Pauling, L. *J. Chem. Phys.* **1936**, *4*, 673. (b) Pople, J. A. *J. Chem. Phys.* **1956**, *24*, 1111.
 (42) (a) London, F. *Proc. R. Soc. London, A* **1937**, *149*, 1937. (b) London, F. *J. Phys. Radium* **1937**, 8397. (c) London, F. *J. Chem. Phys.* **1937**, *5*, 837.
 (43) Boulton, A. J.; Halls, P. J.; Katritzky, A. R. *Org. Magn. Reson.* **1969**, *1*, 311.
 (44) (a) Mullen, K. *Org. Magn. Reson.* **1971**, *3*, 331. (b) Poesche, W. H. *J. Chem. Soc. B* **1966**, 568.
 (45) Jonathan, N.; Gordon, S.; Dailey, B. P. *J. Chem. Phys.* **1962**, *36*, 2443.

(46) Bergmann, E. D., Pullman, B., Eds. "Aromaticity, Pseudo-aromaticity and Anti-aromaticity"; Academic Press: New York, 1971.

allowing this problem to be addressed. Thus the relative ease of reduction of **1**, its low electronic excitation energy, and the high-field ^1H NMR shifts of its peripheral protons are all consistent with its antiaromatic 12- π -electron count.

From a chemical point of view the most appealing evidence for the relative aromaticities of **1** and **2** is the degree of dissociation of the adducts **3** and **4**. Qualitatively, the 14-electron π -system of **2** is more resistant to olefin addition than is the 12-electron π -system of **1**. We can quantify this conclusion if we assume that the entropy changes associated with the two reactions are similar. The difference in the two equilibrium constants is then determined solely by ΔE_{deloc} , the delocalization energy change, for each reaction.⁴⁷ From the expression given in eq 6, the observed K_{diss}

$$-2.303RT \log \frac{K_{\text{diss}}(\mathbf{3},\mathbf{1})}{K_{\text{diss}}(\mathbf{4},\mathbf{2})} = \Delta E_{\text{deloc}}(\mathbf{3},\mathbf{1}) - \Delta E_{\text{deloc}}(\mathbf{4},\mathbf{2}) \quad (6)$$

values translate into a 5 kcal/mol difference in ΔE_{deloc} for the two

(47) Dewar, M. J. S. "The Molecular Orbital Theory of Organic Chemistry"; McGraw-Hill: New York, 1969.

reactions; i.e. **2** is more aromatic than **1** by 5 kcal/mol.

Just as benzene is more aromatic (more resistant to Diels-Alder addition) than naphthalene,⁴⁷ so too is trithiadiazepine itself relative to benzotrithiadiazepine. The former fails to react at all with olefins and undergoes electrophilic substitution typical of a benzenoid aromatic compound.¹²

Acknowledgment. We thank the Natural Sciences and Engineering Research Council of Canada, the Research Corp., the National Science Foundation (EPSCOR Grant ISP 801147), and the State of Arkansas for financial support of this work. We also thank Dr. J. F. Richardson for collecting a low-temperature X-ray data set on **1**.

Registry No. **1**, 34357-13-6; **2**, 97484-08-7; **3**, 100765-34-2; **4**, 100765-35-3; **5**, 22706-22-5; **6**, 273-77-8; $\text{PhN}=\text{S}=\text{NSiMe}_3$, 56839-46-4; Me_3SiNHPH , 3768-55-6; $\text{Me}_3\text{SiN}=\text{S}=\text{O}$, 7522-26-1; SCl_2 , 10545-99-0; 2- $\text{ClSC}_6\text{H}_4\text{SCl}$, 30818-49-6; $\text{Me}_3\text{SiN}=\text{S}=\text{NSiMe}_3$, 88266-99-3; norbornadiene, 121-46-0.

Supplementary Material Available: Listings of anisotropic thermal parameters for **1** (Table S1), **3** (Table S2), and **4** (Table S3) and structure factors for each structure (44 pages). Ordering information is given on any current masthead page.

Contribution from the Department of Chemistry, Victoria University of Wellington, Wellington, New Zealand, and Christopher Ingold Laboratories, University College London, London WC1H 0AJ, United Kingdom

Raman and Resonance Raman Studies of Tetrphosphorus Triselenide

Gary R. Burns,*† Joanne R. Rollo,† and Robin J. H. Clark*†

Received August 8, 1985

The first-order Raman-active phonons of P_4Se_3 have been found to be resonance-enhanced. The Raman band excitation profiles measured at 295 K show broad maxima at $14\,400\text{ cm}^{-1}$, red shifted by $4\,500\text{ cm}^{-1}$ with respect to the absorption edge and by $11\,500\text{ cm}^{-1}$ with respect to the electronic band maximum in solution. A recent redetermination of the crystal structure at 265 K has identified significant selenium-selenium intermolecular contacts that produce a layer lattice in which helical chains of P_4Se_3 molecules are directed along the unit cell a and b axes. It is proposed that the layer lattice confers semiconducting properties on crystalline P_4Se_3 and that the resulting anisotropic resonant transition may be the cause of the enhancement of the Raman-active phonons.

Introduction

The molecules P_4S_3 , P_4Se_3 , As_4S_3 , and As_4Se_3 are the simplest structures found among the large number of cage molecules formed by phosphorus and arsenic with the chalcogen elements sulfur and selenium. Interest in this group of compounds has been stimulated by the growing importance of chalcogenide glasses in current technology.¹ Amorphous chalcogenides are used in fast electrical switches, computer memories, display devices, and television cameras. It is also possible that amorphous films of chalcogenide glasses may be used in the manufacture of layered acoustic wave guides and in the storage of holograms.

P_4S_3 and P_4Se_3 occur as crystalline (α) and plastic (β) modifications, where the latter is characterized by an ordered arrangement of molecules on a lattice but with a high degree of orientational disorder. In this work we shall be mainly concerned with the low-temperature crystalline phase but will make some use of Raman data for the β -phase.

Despite the apparent simplicity of the parent C_{3v} cage (see Figure 1) there is no complete and unambiguous assignment of the normal modes for any of these molecules. Numerous spectroscopic studies²⁻⁶ and a number of normal coordinate treatments⁷⁻¹¹ have failed to characterize the $4a_1 + a_2 + 5e$ normal modes.

The P_4S_3 molecule has received the greatest attention, and there is now a considerable body of information on its Raman- and

infrared-active vibrations. These studies have been aided by the high solubility of P_4S_3 in carbon disulfide and by the greater relative stability of P_4S_3 compared to P_4Se_3 in all phases.

The purposes of this study were to investigate the low-temperature (80 K) Raman spectrum of P_4Se_3 in an attempt to resolve the crystal field and Davydov components of the a_1 and e molecular modes, and to see whether there was any resonance enhancement of the Raman-active vibrations for excitation within the contour of the low-energy absorption band. A toluene solution of P_4Se_3 has an electronic absorption band with a maximum at 387 nm

- (1) Davis, E. A. *Endeavour* **1977**, *1*, 103.
- (2) Bues, W.; Somer, M.; Brockner, W. *Z. Naturforsch., B: Anorg. Chem., Org. Chem.* **1980**, *35B*, 1063 and earlier references therein.
- (3) Chattopadhyay, T.; Carlone, C.; Jayaraman, A.; von Schnering, H. G. *Phys. Rev. B: Condens. Matter* **1981**, *23*, 2471.
- (4) Chattopadhyay, T.; von Schnering, H. G. *Phys. Status Solidi B* **1981**, *103*, 637.
- (5) Chattopadhyay, T.; von Schnering, H. G. *Phys. Status Solidi B* **1981**, *108*, 241.
- (6) Chattopadhyay, T.; Carlone, C.; Jayaraman, A.; von Schnering, H. G. *J. Phys. Chem. Solids* **1982**, *43*, 277.
- (7) Gerding, H.; Marsden, J. W.; Nobel, P. C. *Recl. Trav. Chim. Pays-Bas* **1957**, *76*, 757.
- (8) Cyvin, S. J.; Brunvoll, J.; Cyvin, B. N.; Somer, M.; Brockner, W. *Z. Naturforsch., A: Phys., Phys. Chem., Kosmophys.* **1980**, *35A*, 1062.
- (9) Cyvin, S. J.; Cyvin, B. N.; Somer, M.; Brockner, W. *J. Naturforsch., A: Phys., Phys. Chem., Kosmophys.* **1981**, *36A*, 774.
- (10) Brockner, W.; Somer, M.; Cyvin, B. N.; Cyvin, S. J. *Z. Naturforsch., A: Phys., Phys. Chem., Kosmophys.* **1981**, *36A*, 846.
- (11) Brunvoll, J.; Cyvin, B. N.; Cyvin, S. J. *Z. Naturforsch., A: Phys., Phys. Chem., Kosmophys.* **1982**, *37A*, 342.

* Victoria University of Wellington.

† University College London.